

Thermally assisted hole tunneling at the Au-Si₃N₄ interface and the energy-band diagram of metal-nitride-oxide-semiconductor structures

V. A. Gritsenko* and E. E. Meerson

Institute of Semiconductor Physics, Siberian Branch of the Russian Academy of Sciences, Novosibirsk 630090, Russia

Yu. N. Morokov

Institute of Computational Technologies, Siberian Branch of the Russian Academy of Sciences, Novosibirsk 630090, Russia

(Received 7 July 1997; revised manuscript received 30 October 1997)

Thermally assisted tunneling of holes at the Au-Si₃N₄ interface was experimentally observed. The hole barrier of 1.6 ± 0.2 eV and the effective masses for the hole and electron tunneling into silicon nitride have been determined. A revised energy-band diagram of the metal-nitride-oxide-semiconductor structure is constructed. [S0163-1829(98)52204-7]

The typical values of barriers for an electron and hole injection at semiconductor(metal)-insulator interfaces in MIS (metal-insulator-semiconductor) structures are in the 2–3 eV region. Injection of carriers into insulators of such structures at room temperature is limited by the high field Fowler-Nordheim tunneling mechanism.¹

Forty years ago, the thermally assisted tunneling (TAT) mechanism at a metal-vacuum interface was predicted.² Later, the TAT effect was analyzed for the metal-insulator interface.³ In the TAT mechanism, an electron is excited to some energy by collisions with phonons and then tunnels through a triangle barrier into the conduction or valence bands. TAT from a contact to localized states in polymer⁴ and multiphonon ionization of localized states in insulator and semiconductors^{5–7} was experimentally observed. As far as we know, the direct TAT of carriers from metal into the conduction band or valence band of insulators was not observed experimentally up to now.⁸ The aim of this work is to observe experimentally the TAT effect for holes at the Au/silicon nitride interface.

Amorphous silicon nitride (Si₃N₄) has a high concentration of electron and hole traps and the property to localize injected electrons and holes with a large delocalization time ~ 10 years at 300 K.⁹ According to internal photoemission data, the barriers for electrons and holes at the Si/Si₃N₄ interface are equal and are 2.0 ± 0.1 eV.^{10,11}

The metal-nitride-oxide-semiconductor structures (MNOS) with tunneling-thickness thermal oxide (50 Å) and Si₃N₄ (~ 500 Å) were investigated. The silicon substrates, (100) orientated, with a 7–10 Ohm cm resistivity of *n* and *p* type were used. The Si₃N₄ was deposited with three different methods: method (A) APCVD (atmospheric pressure chemical vapor deposition), SiCl₄/NH₃=0.05, $T=850$ °C, gas carrier H₂; method (B) APCVD, SiCl₄/NH₃=0.01, $T=850$ °C, gas carrier N₂; method (C) LPCVD (lower pressure), SiCl₄/NH₃=0.1, $T=800$ °C. The “natural” oxide on Si₃N₄ was chemically etched before the metal deposition to have reproducible injective contacts to Si₃N₄.¹² The Au and Al contacts were evaporated on Si₃N₄. The injection currents from metals into Si₃N₄ were measured by the impulse polarization of the MNOS structures. Charge trapping kinetics

were determined by the capacitance-voltage (C-V) shift measurements. The different voltage impulse amplitudes and duration were used to study injection mechanisms at different fields at the Si₃N₄-metal interface. The current value was determined by dividing the value of charge trapped in Si₃N₄ by the duration of the voltage impulse. The small values of injected charge were used for current evaluation. This method allows us to separate the electron and hole injection currents from contacts. The details of the method of contact current-voltage characteristic measurements were described earlier.¹² The injection electron currents from Al (*p*-type substrate in accumulation regime by negative potential on Al) and the hole currents from Au (*n*-type substrate in accumulation regime by positive potential on Au) were investigated as functions of the contact field at the Si₃N₄-metal interface at different temperatures.

Control experiments to exclude an injection of carriers from the opposite contact (silicon) into Si₃N₄ were made. By these experiments the conditions when injection of carriers from silicon is negligible were determined. Thus, in the present experiments the injection of electrons from silicon was small at positive potential at Au in comparison with hole injection from Au. Injection of holes from silicon at negative potential at Al was also small in comparison with electron injection from Al.

Increasing the positive polarization impulse duration and amplitude values leads to a shift of the C-V curves to negative voltages due to hole injection from and capturing in Si₃N₄. Three current-voltage characteristics measured at different temperatures are shown in Fig. 1. The experimental hole current-voltage characteristics measured at high temperatures [593 and 523 K] [Fig. 1(a)] are well described by the TAT equation^{2,3}

$$j = CF \exp \left\{ - \left[\Phi - \frac{1}{6} \left(\frac{ehF}{4\pi kT(m^*)^{1/2}} \right)^2 \right] / kT \right\}. \quad (1)$$

Here $C = (2\pi m^* kT)^{1/2} (e/h)^2$, j is the current density, Φ is the barrier energy, m^* is the effective mass, and F is the electric field. The hole barrier value $\Phi_h = 1.6 \pm 0.2$ eV has been determined by extrapolation of $\lg(j/F)$ lines in Fig. 1(a) to the zero field. The slope of the current-voltage depen-

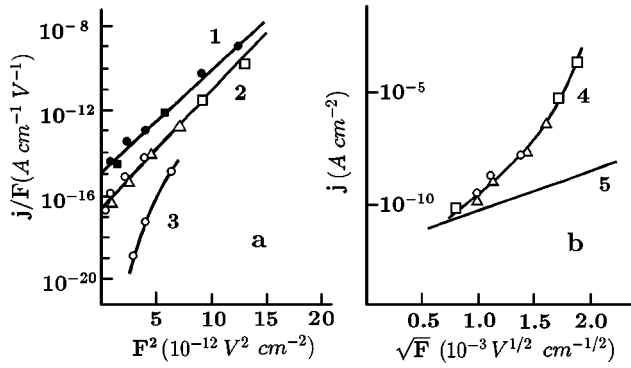


FIG. 1. The hole current–nitride contact field relationship at different temperatures at Au/Si₃N₄ interface: (a) coordinates correspond to the TAT; (b) coordinates correspond to the Schottky effect. Si₃N₄ was produced with the different methods: circles, method (A); squares, method (B); triangles, method (C). Curves: 1, $T=593$ K; 2, 4, 523 K; 3, 77 K; 5, theoretical Schottky curve for 523 K.

dence gives the value for the hole effective mass $m_h^*/m_0 = (0.3 \pm 0.1)$ in Si₃N₄. Here m_0 is the free electron mass. The Schottky mechanism predicts an exponential dependence of the current on the field and temperature²

$$j = AT^2 \exp \left[- \frac{(\Phi - \beta_{sh} F^{1/2})}{kT} \right]. \quad (2)$$

$$A = 4\pi m^* k^2 e / h^3 = 120(m^*/m_0) A / (\text{cm}^2 \text{K}^2),$$

$$\beta_{sh} = \sqrt{e^3 / (4\pi\epsilon_0\epsilon_\infty)}.$$

Here, ϵ_∞ is the high frequency dielectric permittivity.

The experimental curve measured at 523 K is not described by the Schottky mechanism [Fig. 1(b)]. The TAT effect was observed experimentally in the MNOS structures with Si₃N₄ evaporated by different methods. So, the TAT mechanism and the parameters Φ_h and m_h^* reflect the fundamental properties of the Au–Si₃N₄ interface and silicon nitride.

The low temperature (room and liquid nitrogen) current-voltage characteristics are not described by TAT or the Schottky law [Fig. 1(a)]. In the region from room to liquid nitrogen temperature, the hole current depends weakly on temperature. The hole injection is described by the tunneling Fowler-Nordheim mechanism at room and liquid nitrogen temperatures^{1,2,8} (Fig. 2)

$$j = BF^2 \exp[-D(m^*\Phi^3)^{1/2}/F]. \quad (3)$$

$$B = e^3 / (8\pi\hbar\Phi), \quad D = 8\pi\sqrt{2} / (3\hbar e).$$

A slope of lines $\lg(j/F^2)$ versus $1/F$ gives the value $(m_h^*/m_0)^{1/2}\Phi_h^{3/2} = 1.2 \text{ eV}^{3/2}$. For $\Phi_h = 1.6 \text{ eV}$, the hole effective mass is $m_h^*/m_0 = 0.35$. This value well agrees with one obtained at 593 and 523 K in the TAT region.

A similar analysis was made for electrons injected from Al into Si₃N₄. An electron injection from Al at 300 and 77 K is temperature independent and is described by the Fowler-Nordheim mechanism (Fig. 2). The parameter $(m_e^*/m_0)\Phi_e^{3/2}$ determined from Fig. 2 is $1.87 \text{ eV}^{3/2}$. The electron injection

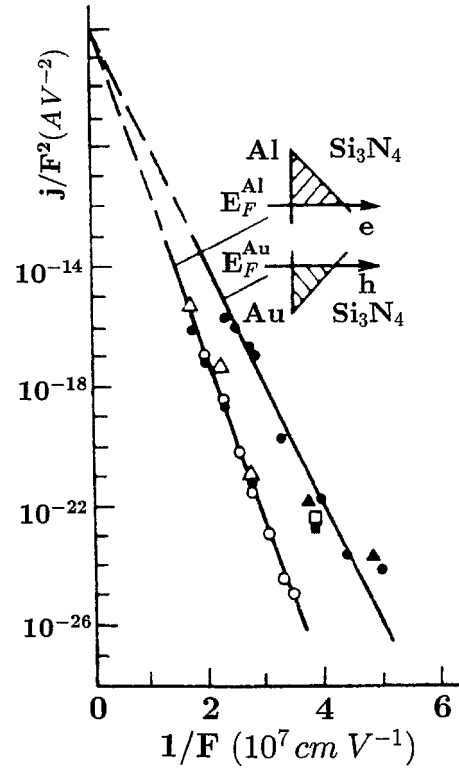


FIG. 2. The hole and electron tunneling current–nitride contact field relationship for electron (Al–Si₃N₄) and hole (Au–Si₃N₄) injection. The dots correspond to various methods of the Si₃N₄ deposition, as noted in Fig. 1.

current does not depend on the evaporation method. The value $m_e^*/m_0 = 0.4$ was obtained using the electron barrier $\Phi_e = 2.0 \text{ eV}$ determined^{10,11,13} for electrons at the Si–Si₃N₄ interface.

In this work, the TAT mechanism and the tunneling of holes and electrons are interpreted in terms of tunneling through a triangular barrier. The influence of image forces was neglected in the analysis. It has been shown that the influence of classical image forces is small in photon-assisted tunneling.¹⁴

The barrier energy at the Au–Si₃N₄ interface $\Phi_h = 1.6 \text{ eV}$ obtained by TAT is the same as the value obtained by XPS.^{15,16} The difference of the work functions for Au and Al measured by the C–V method in the MNOS structures investigated is $0.9 \pm 0.1 \text{ eV}$. This value agrees with the value of 0.9 eV obtained by C–V in the photoinjection method for the Si–SiO₂ interface.¹⁷

The gap in Si₃N₄ determined in the electron and hole injection experiments of the present work is $2.1 + 1.6 + 0.9 = 4.6 \text{ eV}$. This value is 0.5 eV lower than the “optical” gap $E_g = 5.1 \text{ eV}$ obtained from optical absorption using the Tauz model.^{10,11,13,18} According to the obtained values of barriers at the Au–Si₃N₄ interface, the hole barrier at the Si–Si₃N₄ interface is 1.5 eV for $E_v = 5.1 \text{ eV}$ for silicon (Fig. 3). This value is 0.6 eV lower than the barrier value obtained from the internal photoemission experiments.^{10,11}

The obtained values of the electron effective masses, $m_e^* = 0.4m_0$, in silicon nitride agree with the value of an electron tunneling mass of $0.6m_0$ obtained by a resonant tunneling experiment¹⁹ for Si₃N₄:H and the silicon dioxide electron effective mass $m_e^*/m_0 = 0.4$.^{1,20} Earlier, the values

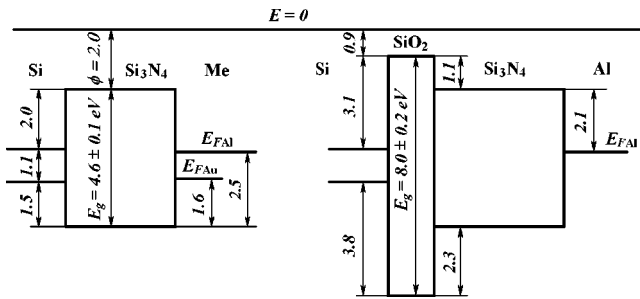


FIG. 3. The energy-band diagram of the MNS and MNOS structures with different metals obtained by injection of electrons and holes into Si_3N_4 . Zero of energy corresponds to the free electron energy in vacuum.

$m_e^*/m_0 = (0.05-0.13)$ and $m_h^*/m_0 = 0.05$ for Si_3N_4 were obtained by charging of Si_3N_4 from silicon.²¹ These anomalous small masses were evaluated due to an existence of the tunneled thin oxide layer between Si and Si_3N_4 . The overestimated value of the hole barrier obtained from photoemission experiments, $\Phi_h = 2.0$ eV, is the reason of some unexpected anomalies obtained by hole injection from silicon in Si_3N_4 .^{22,23}

The energy-band diagram of the MNOS structure was constructed (Fig. 3) taking into account the work functions

$\phi(\text{Au}) = 5.0$ eV and $\phi(\text{Al}) = 4.1$ eV. According to Fig. 3, the barrier at Si- Si_3N_4 interface for holes is 0.5 eV lower than for electrons. This difference explains the dominant hole conduction of Si_3N_4 by the negative potential on the metal.^{15,24}

The band calculation of Si_3N_4 ²⁵ gives the value of the hole mass, $m_h^*/m_0 = 3.0$. This heavy hole mass is related to the narrow band of the N $2p_\pi$ nonbonding orbitals. These orbitals give the electronic states near the top of the Si_3N_4 valence band. But the experiment and the last numerical simulation of the Si_3N_4 electronic structure show that there are not only the N $2p_\pi$ nonbonding orbitals, but the Si $3s, 3p$ -N $2p, 3s$ bonding orbitals too²⁶ at the Si_3N_4 valence band top. Light holes obtained in this work correspond to the wide band of the bonding states. In terms of band theory, the valence band of crystalline Si_3N_4 is degenerate. This result was obtained by the recent band calculations for Si_3N_4 .²⁵

In conclusion, the thermally assisted tunneling of holes from a metal into the valence band of an insulator was for the first time experimentally observed. The hole effective masses for Si_3N_4 have been determined for the first time. The hole barrier value at the Au- Si_3N_4 interface has been determined and a more realistic (than from the photoemission experiments) energy band diagram of the MNS and MNOS structures has been constructed.

*Present address: Electronic Engineering Department, The Chinese University of Hong Kong, Shatin, N.T., Hong Kong. Electronic address: vladimir@ee.cuhk.edu.hk

¹J. Maserjian and N. Zamani, J. Appl. Phys. **53**, 559 (1982).

²E. L. Murphy and R. H. Good, Jr., Phys. Rev. **102**, 1464 (1956).

³G. G. Roberts and J. I. Polanco, Phys. Status Solidi A **1**, 409 (1970).

⁴M. A. Abkowitz, H. A. Mizes, and J. S. Facci, Appl. Phys. Lett. **66**, 1288 (1995).

⁵R. M. Hill, Philos. Mag. **23**, 59 (1971).

⁶V. A. Gritsenko, Ya. O. Roizin, L. E. Semenshuk, and N. L. Shwarz, Solid State Commun. **38**, 351 (1981).

⁷V. N. Abakumov, I. A. Merkulov, V. I. Perel, and I. N. Yasievich, Zh. Eksp. Teor. Fiz. **89**, 1472 (1985) [Sov. Phys. JETP **62**, 853 (1985)].

⁸A. Modinos, *Field, Thermionic and Secondary Electron Emission Spectroscopy* (Plenum, New York, 1984).

⁹V. A. Gritsenko, in *Silicon Nitride in Electronics*, edited by A. V. Rzhano (Elsevier, New York, 1988).

¹⁰A. M. Goodman, Appl. Phys. Lett. **13**, 275 (1968).

¹¹D. J. DiMaria and P. C. Arnett, Appl. Phys. Lett. **26**, 711 (1975).

¹²V. A. Gritsenko and E. E. Meerson, Mikroelektron. **17**, 249 (1988).

¹³V. A. Gritsenko, N. D. Dikovskaya, and K. P. Mogilnikov, Thin Solid Films **51**, 353 (1978).

¹⁴Z. A. Weinberg and A. Hartstein, Solid State Commun. **20**, 179 (1976).

¹⁵Z. A. Weinberg and R. A. Pollak, Appl. Phys. Lett. **27**, 254 (1975).

¹⁶V. A. Gritsenko, *Atomic and Electronic Structure of Amorphous Insulators in Silicon MIS Structures* (Science, Novosibirsk, 1993).

¹⁷S. M. Sze, *Physics of Semiconductor Devices* (Wiley-Interscience, New York, 1981).

¹⁸N. F. Mott and E. A. Davis, *Electron Processes in Non-Crystalline Materials* (Clarendon Press, Oxford, 1979).

¹⁹S. Miyazaki, Y. Ihara, and M. Hirose, Phys. Rev. Lett. **59**, 125 (1987).

²⁰M. Lenzlinger and E. H. Snow, J. Appl. Phys. **40**, 278 (1979).

²¹P. C. Arnett and D. J. DiMaria, J. Appl. Phys. **47**, 2092 (1976).

²²M. J. Powell, Appl. Phys. Lett. **43**, 597 (1983).

²³V. I. Koldjaev and K. K. Svitashv, Mikroelektron. **15**, 255 (1986).

²⁴A. S. Ginovker, V. A. Gritsenko, and S. P. Sinita, Phys. Status Solidi A **26**, 489 (1974).

²⁵Y. Xu and W. Y. Ching, Phys. Rev. B **51**, 17 379 (1995).

²⁶V. A. Gritsenko, Yu. N. Morokov, and Yu. N. Novikov, Appl. Surf. Sci. **113/114**, 417 (1997).